ℰ

Non-Abelian dark matter and dark radiation

Manuel A. Buen-Abad,[*] Gustavo Marques-Tavares,[†] and Martin Schmaltz[‡]

Physics Department, Boston University, 590 Commonwealth Avenue, Boston, Massachusetts 02215, USA
(Received 5 June 2015; published 27 July 2015)

We propose a new class of dark matter models with unusual phenomenology. What is ordinary about our models is that dark matter particles are weakly interacting massive particles; they are weakly coupled to the standard model and have weak scale masses. What is unusual is that they come in multiplets of a new dark non-Abelian gauge group with milliweak coupling. The massless dark gluons of this dark gauge group contribute to the energy density of the Universe as a form of weakly self-interacting dark radiation. In this paper we explore the consequences of having (i) dark matter in multiplets, (ii) self-interacting dark radiation, and (iii) dark matter which is weakly coupled to dark radiation. We find that (i) dark matter cross sections are modified by multiplicity factors which have significant consequences for collider searches and indirect detection, and (ii) dark gluons have thermal abundances which affect the cosmic microwave background (CMB) as dark radiation. Unlike additional massless neutrino species the dark gluons are interacting and have vanishing viscosity and (iii) the coupling of dark radiation to dark matter represents a new mechanism for damping the large scale structure power spectrum. A combination of additional radiation and slightly damped structure is interesting because it can remove tensions between global ΛCDM fits from the CMB and direct measurements of the Hubble expansion rate (H_0) and large scale structure (σ_8).

I. INTRODUCTION

Dark matter (DM) makes up more than 80% of the matter content of our Universe [1]. Despite the overwhelming quantitative evidence for cold dark matter (CDM) from its gravitational interactions, and its inclusion in the standard ΛCDM cosmological model, we only have very limited information about possible nongravitational interactions of DM. Existing upper bounds on interactions between the DM and the standard model (SM) and self interactions of the DM leave a broad range of possibilities for models of DM. Viable models may include a whole dark sector consisting of different species of particles which interact only with themselves and with DM (see e.g. [2–4]). Furthermore, there is some tension between the best fit parameters in ΛCDM as inferred from the cosmic microwave background (CMB) [1], and direct measurements of H_0 using standard candles and σ_8 using galaxy clusters [5–7]. While it is premature to draw definite conclusions about these discrepancies, they motivate the study of interacting dark sectors which go beyond the ordinary cold dark matter of ΛCDM.

In this work, we propose a novel scenario for an interacting dark sector which predicts several important modifications to standard CDM phenomenology. Our dark

sector includes a weakly interacting massive particle (WIMP) as the dark matter. As usual, weak interactions between the DM and the SM keep the two sectors in equilibrium at high temperatures and set the abundance of DM through thermal freeze-out. The nontrivial new ingredient of our scenario is that the DM particles are charged under a new non-Abelian dark gauge group.[1] Thus our dark sector consists of a degenerate multiplet of massive DM particles coupled to dark radiation (DR) in the form of massless non-Abelian gauge bosons. Observations of large scale structure tightly constrain long-range interactions of DM with dark radiation and require very small gauge couplings,[2] $g_d < 10^{-3}$, so that the dark confinement temperature is well below the current CMB temperature.[3] Thus confinement in the dark sector is irrelevant, and the "dark gluons" are a thermal bath of weakly coupled massless particles which is well described as a perfect fluid. Note that this is distinct from neutrinos which free-stream and are therefore not a perfect fluid. The two types of dark

---

[*]buenabad@bu.edu
[†]gusmt@bu.edu
[‡]schmaltz@bu.edu

[1]New visible particles charged under a new non-Abelian gauge group with macroscopic sized confinement scale have been proposed in the past under the name of theta-particles [8–10] and more recently as quirks [11].
[2]Such couplings are too small to have appreciable effects on the bullet cluster, the shape of galactic dark matter halos, or DM protohalos. They are also too small to have any bearing on the "core vs cusp" or "missing satellites" problems.
[3]For recent discussions of non-Abelian dark sectors in a different context see [12–17].

radiation can be distinguished through their imprints on the CMB [18,19].

The general features of our dark sector lead to several distinct observable effects which can be broadly classified as due to (i) multiplicity of the dark matter, (ii) dark radiation in the form of the dark gluon fluid, and (iii) interactions between DM and dark radiation. We briefly summarize the salient features of each of the three effects here. Details will be provided in subsequent sections.

(i) DM multiplicity: Being charged under an unbroken non-Abelian gauge group, DM particles come in degenerate multiplets of N dark colors. This multiplicity leads to several easy-to-understand but important differences from conventional WIMPs. First off, DM annihilation cross sections (into SM particles) are suppressed by $1/N$ from averaging over initial states. Assuming thermal freeze-out, we predict that our dark matter mass is smaller by a factor of $1/\sqrt{N}$ than in models without dark matter multiplicity. Similarly, indirect detection bounds from dark matter annihilation into photons near the Galactic center are relaxed because of the $1/N$ in the annihilation cross section. Second, DM pair production cross sections at colliders are enhanced by a factor of N from the multiplicity of possible final states. Third, direct detection bounds for DM are unchanged because the scattering cross section for DM particles off nuclei does not contain multiplicity factors. We discuss these effects, which would also follow from a non-Abelian global symmetry, in Sec. III.

(ii) Dark radiation: Through their interactions with the DM, dark gluons come into thermal equilibrium with the SM in the early Universe. After freeze-out of the DM the dark gluons decouple from the SM. They maintain a thermal distribution but end up cooling relative to the CMB because the photons are heated by absorbing the entropy contained in massive SM particles. The dark gluons are observable through their contribution to the radiation density in the Universe, an effect which is conventionally expressed in terms of an effective number of neutrino species (see [20] for a recent discussion of bounds on new relativistic degrees of freedom from the CMB). We find $\triangle N_{\text{eff}} \sim 0.07(N^2 - 1)$ for the $N^2 - 1$ gluons of an $SU(N)_d$ gauge group. Bounds on N_{eff} from Planck and from nucleosynthesis give $N < 4$ at 95% confidence level. An increase in the radiation density also shifts the best fit values of other cosmological parameters from the CMB. The two most significant shifts are increases in the predicted values of H_0 and σ_8. An increase of H_0 would remove the tension between CMB fits and direct measurements of H_0. An increase in σ_8 worsens the tension between CMB data and direct

observations of σ_8 from large scale structure. However, as discussed in the next item, interactions between DM and dark gluons can remove this tension. Finally, the fact that dark gluons are self interacting allows one to distinguish them from additional neutrino species. Dark gluons are well described by a perfect fluid with no viscosity and therefore lead to less damping of the CMB power spectrum in comparison to extra free-streaming relativistic fluids. Future CMB data will be precise enough to determine the viscosity of any significant new component of dark radiation and can therefore distinguish between additional neutrinos and dark gluons [19]. We elaborate on the phenomenology of our dark radiation in Sec. IV.

(iii) DM—dark radiation interactions: Scattering of DR off DM introduces a drag force between the non-relativistic DM fluid and the relativistic radiation. This drag suppresses gravitational clustering and is therefore observable in the matter power spectrum. Allowing for matter perturbations to grow at least approximately as in ΛCDM gives a conservative upper bound of $\alpha_d \lesssim 10^{-8}$. What we find particularly interesting about our scenario is that the momentum transfer cross section for DM-DR scales with temperature like the Hubble parameter during radiation domination. This means that the effect of the radiation remains equally important throughout radiation domination, leading to a smooth reduction of the power spectrum. This is in contrast with the more frequently studied case where the DM interactions freeze out at a critical temperature, leading to a sharp cutoff in the power spectrum at small scales [3,21–23]. We show that a very small and smooth reduction of the power spectrum may resolve the tension in the indirect determination of σ_8 from Planck data and direct measurements of the power spectrum at large scales (see e.g. [1,6,7]). We discuss DM-DR interactions in Sec. V.

Most of the features associated with non-Abelian dark matter are expected to hold in a broad class of models irrespective of the specific interactions between the DM and the SM. However, in the interest of concreteness and for clarity of presentation we focus on a specific example model which is described in Sec. II. The DM in the model is a "winolike" $SU(2)_{\text{weak}}$ triplet Dirac fermion which transforms as a fundamental under a dark $SU(N)_d$ gauge group.

II. THE MODEL AND DM THERMAL RELIC ABUNDANCE

For concreteness we focus on a specific realization of a non-Abelian dark matter. We take the dark matter particle to be a Dirac fermion in the $(1, 3)_0$ representation of the standard model $(SU(3), SU(2))_{U(1)}$ gauge group and in the

fundamental representation of dark $SU(N)_d$. It has an $SU(2)_{weak}$ preserving Dirac mass M_χ and no additional interactions with the standard model besides gauge interactions. Electroweak symmetry breaking leads to a loop-induced mass splitting between the charged and neutral components of the $SU(2)_{weak}$ triplet. In the limit $M_\chi \gg M_W$ the splitting is independent of M_χ and given by [24,25]

$$\delta M_\chi = M_{\chi^\pm} - M_{\chi^0} \approx 0.16 \text{ GeV.} \tag{1}$$

The neutral component χ^0 is the lightest particle which carries fundamental $SU(N)_d$ charge and is therefore stable; it is our DM candidate. From the perspective of SM interactions the dark $SU(N)_d$ is simply a global symmetry, so that our DM acts like N identical copies of a weakly interacting particle χ^0 with Dirac mass M_χ. In the following, we determine M_χ by requiring that the correct DM abundance is obtained from thermal freeze-out.

At the time of DM chemical freeze-out $T \sim M_\chi/26 \gg \delta M_\chi$ so that we can ignore the mass splitting between the different components of χ^a when calculating relic abundances. Once the temperature drops below δM_χ, the charged $\chi^\pm$ decay to χ^0 plus standard model particles. Thus the (comoving) number density of χ^0 particles at low temperatures is simply given by summing over all components of χ^a at DM freeze-out, i.e. $\sum_a n_{\chi^a} \rightarrow n_{\chi^0}$. This explains why we can use the abundance calculation for the whole triplet χ^a in order to find the DM relic abundance.

We show in subsequent sections that cosmology requires the dark gauge coupling to be much smaller than the SM gauge couplings. Therefore the relevant interactions for the thermal relic calculations are of the form $\chi\chi \rightarrow$ SM and independent of the dark gauge coupling. Figure 1 shows some of the relevant diagrams for DM annihilating to SM particles. In the limit $M_\chi^2 \gg M_W^2$, the thermally averaged effective annihilation cross section is

$$\langle \sigma v \rangle = \frac{1}{2N} \frac{37 g_2^4}{192\pi M_\chi^2}, \tag{2}$$

where g_2 is the $SU(2)_{weak}$ gauge coupling. This cross section differs from the standard $SU(2)_{weak}$ triplet wino [26] by the extra $1/2N$ factor, which comes from the

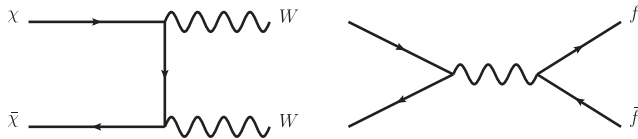FIG. 1. Annihilation of dark matter into $SU(2)_{weak}$ gauge bosons or SM fermions. Since the mass splitting between members of $SU(2)_{weak}$ multiplets is small compared with energy transfer in the annihilation diagrams (i.e. twice the χ mass) we compute the coannihilation of full $SU(2)_{weak}$ multiplets and ignore the mass splittings.

TABLE I. Dark matter masses required to get the correct thermal abundance as a function of N.

$N = 2$	$N = 3$	$N = 4$	$N = 5$	Generic N
1.2 TeV	1.0 TeV	0.9 TeV	0.8 TeV	$\sim 2.4/\sqrt{2N}$ TeV

multiplicity associated with the $SU(N)_d$ representation and the fact that χ is a four-component Dirac fermion instead of a two-component Majorana fermion. The $1/2N$ factor can be easily understood from the fact that any given DM particle carries a dark color charge and can only annihilate if it finds an antiparticle with the corresponding antidark color, thus reducing the color averaged annihilation cross section.

If the DM abundance is set by thermal freeze-out, then—to a good approximation—the DM mass density today depends on the DM mass only through its annihilation cross section [27]. Therefore, holding the cross section in Eq. (2) fixed at the cosmologically preferred value we see that the mass required to get the correct relic abundance decreases as the square root of N. In Table I we give the mass of DM for different values of N using the tree level annihilation cross section. The masses are significantly lower than for the usual wino case where the tree level formula predicts a mass of 2.4 TeV.[4]

III. DARK MATTER MULTIPLICITY AND EXPERIMENTAL SEARCHES

As will be discussed in subsequent sections, astrophysical and cosmological constraints require very small dark gauge couplings of order $\alpha_d < 10^{-8}$. This is too small to have observable effects for production of DM at colliders, or for direct or indirect detection of DM. However, it is important to take into account that DM particles are in multiplets of the dark $SU(N)_d$, i.e. there are multiplicity factors associated with DM processes. In the previous section we already discussed that the predicted mass for our thermal relic DM is reduced by a multiplicity factor of $1/\sqrt{2N}$, which can lead to large changes in sensitivity of experimental searches. Similar multiplicity/color factors also appear in cross sections associated with DM detection. Figure 2 shows the color factors associated with the different kinds of DM searches. In what follows we briefly describe the effects of $SU(N)_d$ multiplicity for direct and indirect detection and also for collider searches for DM.

---

[4]In the case of the wino, the preferred mass is close to a Sommerfeld resonance of the weak interactions and one must account for Sommerfeld enhancement to obtain $M_{wino} \simeq 3$ TeV [28]. In our case, the DM mass is safely below the Sommerfeld resonances and the perturbative annihilation formula (2) is adequate.
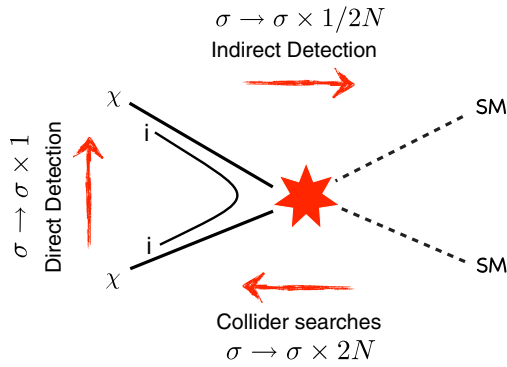
FIG. 2 (color online). Color factors for the different types of DM search experiments. The different multiplicity factors can be easily understood from the color flow in the figure. For direct detection the color of the incoming dark matter is the same as of the outgoing and so there is no multiplicity factor. For indirect detection it is an annihilation diagram, so just as for the thermal relic calculation there is a $1/2N$ suppression because a DM particle can only annihilate if it finds the antiparticle with the right antidark color. For colliders there is a $2N$ enhancement because any of the different N colors can be created and an extra two from Dirac vs Majorana.

A. Direct detection

For direct detection there is no color factor associated with the multiplicity; thus the only change comes from dark matter being lighter. The spin-independent cross section for dark matter scattering of the nucleus is approximately 10^{-47} cm^2, and independent of the DM mass as long as $M_\chi \gg M_W$ [29]. This cross section is an order of magnitude smaller than the projected sensitivity of the next generation direct detection experiments [30]. However, in the mass range of interest (around 1 TeV) it is above the neutrino background and potentially within reach of future experiments.

B. Indirect detection

The annihilation cross section relevant for indirect detection is suppressed by a $1/2N$ factor. Taking into account Sommerfeld enhancement the cross section is further reduced relative to the standard wino model. This is because there is a resonant Sommerfeld enhancement from weak interactions for dark matter masses in the 2–3 TeV range, but the enhancement is much smaller for masses around 1 TeV. The wino model has been investigated recently [31–35], and is strongly disfavored by H.E.S.S. data. Our $SU(N)_d$ model is not yet constrained by either H.E.S.S. or Fermi data for any $N \geq 2$, but the annihilation cross section is close to H.E.S.S. sensitivity as shown in Fig. 3. It is worth noting that the limits shown in Fig. 3 assume a specific Navarro-Frenk-White profile and there is a large uncertainty in these limits due to our limited knowledge of the dark matter distribution in the center of the galaxy. Also shown in the figure is the projected reach
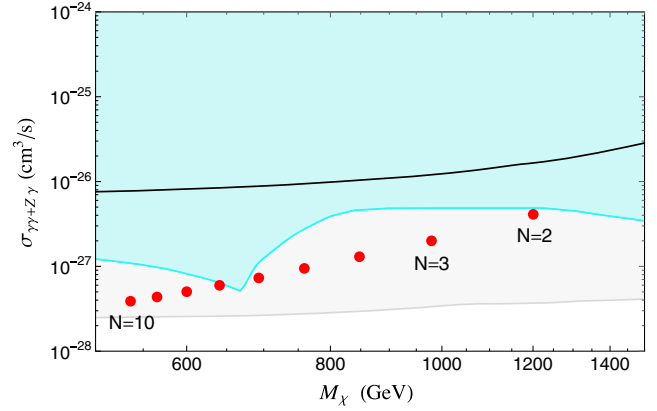

FIG. 3 (color online). Indirect detection constraints from gamma ray line searches from H.E.S.S. (blue region) and projected sensitivity for gamma ray lines at CTA (gray region) assuming an Navarro-Frenk-White profile for the dark matter distribution in the Galactic center, both taken from [34]. The red dots are the cross sections for dark matter annihilation into gamma rays in our models for $N = 2$ up to $N = 10$, which were obtained by appropriately rescaling the next-to-leading-log cross section with Sommerfeld enhancement from [34]. For comparison we plotted in black the cross section for the annihilation cross section to photons in the standard wino model as a function of mass, also from [34].

of CTA [36], assuming five hours of observation time. One can see that CTA should have enough sensitivity to discover or rule out our model up to at least $N = 10$, and therefore is the most promising search for discovering dark matter in our model.

C. LHC and future collider searches

The multiplicity factor enhances sensitivity of collider searches to our DM in two ways. Most importantly, the predicted DM mass from thermal freeze-out is lowered, and thus a lower partonic center of mass energy is required to pair produce DM at a collider. For example, at the 14 TeV LHC and for DM masses near $M_{DM} \sim 500$ GeV the DM cross section scales as $(1/M_{DM})^6$ because of the strong energy dependence of the parton luminosities. In addition, the cross section for pair producing dark matter is enhanced by the final state multiplicity factor $2N$.

In the left panel of Fig. 4 we show the expected sensitivity of the high luminosity LHC to the DM in our model. The solid dots correspond to DM with multiplicity N and Dirac masses chosen so that the correct thermal DM abundance is obtained. We see that the 14 TeV LHC is sensitive to DM with $N \geq 7$. For comparison, we also show the expected sensitivity to a standard wino $SU(2)_{weak}$ triplet with a Majorana mass. Note that the wino has the correct thermal abundance only for $M_{wino} \simeq 3$ TeV. Existing monojet searches from ATLAS [37] and CMS [38] with 8 TeV collisions and a luminosity of 19.5 fb^{-1} already rule out $N \gtrsim 20$.
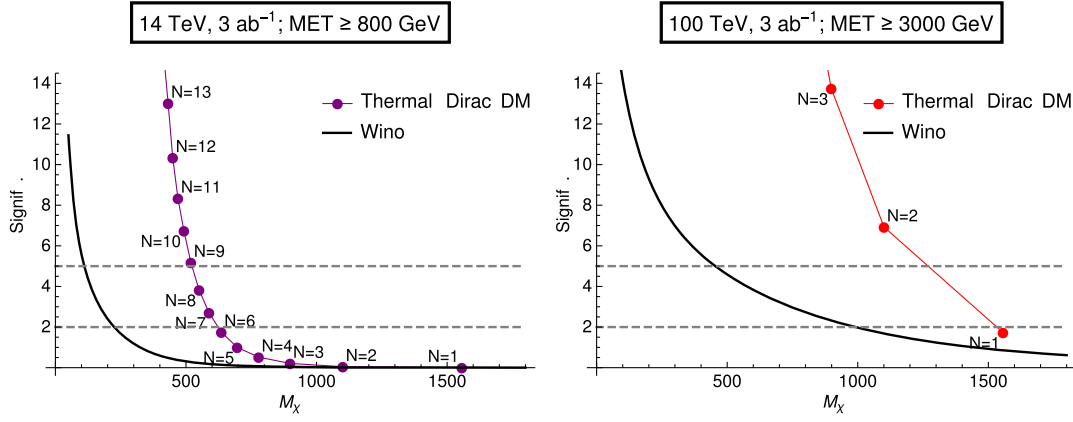
FIG. 4 (color online).   Expected significance of missing energy (MET) searches for DM at the LHC and a future 100 TeV collider. The solid black lines in each plot correspond to the sensitivity of the collider to winolike DM, an $SU(2)_{\text{weak}}$ triplet Majorana fermion. The colored dots labeled by different N values correspond to our models in which the DM is a Dirac fermion with multiplicity N and mass chosen to yield the correct abundance from thermal freeze-out.

In the right panel we show that a 100 TeV future collider can discover our DM above backgrounds even for the smallest non-Abelian multiplet of $N = 2$ and perhaps may be able to rule out a Dirac wino. The significances for these plots were determined from parton level signal and background events which were computed with MadGraph [39]. The main irreducible backgrounds are due to jets plus Z or W with MET from decays to neutrinos. We computed signal and backgrounds to leading order ($\alpha_s\alpha_W$) and assumed that the experiments will be able to limit background systematic uncertainties to 2%. For the wino, our results are consistent with the more sophisticated studies in [40,41]. These references also showed that a MET plus "disappearing track" search for the production of $\chi^{\pm}$ can improve sensitivity because it is free of irreducible SM backgrounds.

Another observable consequence of this model is a change in the running of the electroweak gauge coupling [42]. The multiplicity of DM leads to a $2N$ enhancement factor in the DM contribution to running of α_W at one loop, which would be observable at the proposed 100 TeV hadron colliders.

IV. DARK GLUONS AS DARK RADIATION

In this section we turn our attention to the cosmic evolution of the energy density in dark gluons and its effects on the CMB. An important parameter which determines the effects of dark gluons on the CMB is the ratio of temperatures of the dark gluon plasma T_d over the photon temperature T.

Dark gluons are coupled to the thermal bath of SM particles through their couplings to the DM which is in equilibrium with the SM in the early Universe. If α_d is not too small the dark gluons also equilibrate with the SM plasma at early times, so that $T_d = T$ before DM freeze-out. To determine the smallest possible coupling α_d for

which the dark gluons are in chemical and kinetic equilibrium with the SM we consider the Feynman diagram in Fig. 5. At temperatures higher than M_χ, the thermally averaged cross section for this process times the DM number density is given by

$$n_\chi\langle\sigma v\rangle \sim T^3 \frac{\pi\alpha_W\alpha_d}{T^2}. \tag{3}$$

Comparing this to the Hubble rate H we find that the dark gluons are in equilibrium with the SM at $T \sim M_\chi$ for

$$\alpha_d \gtrsim \frac{1}{\alpha_W}\frac{M_\chi}{M_{\text{Planck}}}.$$

Thus even for α_d as small as 10^{-13} the dark gluons come to chemical and thermal equilibrium with the SM at temperatures of order M_χ. However, when the Universe cools below $T \sim M_\chi$ dark matter becomes nonrelativistic and its number density drops exponentially. Then the rate for the process in Fig. 5 becomes[5]

$$n_\chi\langle\sigma v\rangle \sim (M_\chi T)^{3/2} e^{-M_\chi/T}\frac{\pi\alpha_W\alpha_d}{M_\chi^2}, \tag{4}$$

and the dark gluons decouple at temperatures of about M_χ for $\alpha_d \sim 10^{-13}$ to about $M_\chi/20$ for $\alpha_d \sim 10^{-3}$. Below the decoupling temperature the dark radiation fluid evolves independently with a temperature T_d which redshifts as $1/a$.

The temperature of the photon fluid also redshifts as $1/a$ for most of the Universe's evolution. However, when massive SM particles become nonrelativistic they

---

[5]Note that for temperatures below the W mass, the W boson in Fig. 5 should be replaced by a photon and the α_W in Eq. (4) by α_{em}.
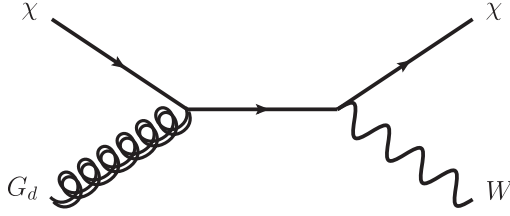
FIG. 5. The process through which dark gluons maintain equilibrium with the DM and the SM plasma for small α_d.

annihilate into the remaining lighter SM particles which effectively heats up the photons compared to the dark gluons (similarly to what happens to photons and neutrinos after neutrino decoupling [27]). The ratio between the photon and dark gluon temperatures can be easily calculated in the instantaneous decoupling approximation by requiring that the entropy per comoving volume is conserved independently in each fluid,

$$\frac{T_d}{T_\gamma} = \left(\frac{g_*^f}{g_*^i}\right)^{1/3}, \qquad (5)$$

where g_*^i is the number of effective degrees of freedom in the SM plasma at the time of dark gluon decoupling and g_*^f the number of effective degrees of freedom at any later time.

The CMB places strong constraints on the energy density in relativistic particles at the time of recombination. This constraint is usually presented in terms of the number of effective neutrino species, $N_{\rm eff}$. The contribution of the dark gluons to $N_{\rm eff}$ is given by

$$\Delta N_{\rm eff} = \frac{8}{7}(N^2 - 1)(T_d/T_\nu)^4, \qquad (6)$$

where the $N^2 - 1$ is the number of generators of $SU(N)_d$ and T_ν is the neutrino temperature. The ratio can be calculated using Eq. (5) right at neutrino decoupling when neutrino and photon temperatures are still the same. Assuming that the decoupling between dark gluons and the SM happens at temperatures around 50 GeV one finds

$$\Delta N_{\rm eff} = 0.07(N^2 - 1).$$

The strongest constraint on $N_{\rm eff}$ comes from the 2015 Planck data [1], which found $N_{\rm eff} = 3.15 \pm 0.46$ at 95% confidence to be compared with the SM prediction [43] $N_{\rm eff}^{\rm SM} = 3.046$. We see that this rules out $N \geq 4$ and that $N = 3$ is within the 2σ allowed range. However, we note that the Planck analysis assumes the ΛCDM model with one additional parameter, $N_{\rm eff}$. This limit could potentially be relaxed in our scenario where there are important differences as we will now discuss.

The effects of dark radiation can be divided into so-called background effects and perturbation effects. Background effects are due to a change in the average energy density in relativistic degrees of freedom and are not sensitive to any other properties of the dark radiation fluid. The largest background effect of extra radiation from relativistic degrees of freedom is to change the redshift of matter-radiation equality $z_{\rm eq}$. Since $z_{\rm eq}$ is very well measured a fit to the data is forced to maintain the redshift of matter-radiation equality by simultaneously increasing the dark matter density (see e.g. [44–46]). This change in the matter density in turn requires a change in the Hubble parameter today H_0, in order to keep Ω_m fixed (the ratio between the matter density and the critical density). Thus we see that a fit to the CMB data alone has an approximate flat direction in which an increase in $N_{\rm eff}$ can be compensated for by simultaneous increases in $\rho_{\rm DM}$ and H_0.

The perturbation effects are due to perturbations in the dark radiation fluid and thus sensitive to properties of dark radiation. In particular there are two additional parameters which distinguish different types of dark radiation; see e.g. [19]: the effective sound speed $c_{\rm eff}^2$ and the viscosity speed $c_{\rm vis}^2$. The dark gluons are a relativistic fluid and have $c_{\rm eff}^2 = 1/3$, the same as for neutrinos. However—unlike neutrinos—the dark gluons have self interactions which come from the non-Abelian gauge kinetic terms. If the rate of dark gluon-gluon scattering is large compared to the Hubble parameter then the dark gluons are well described as an ideal fluid instead of a free-streaming fluid as for neutrinos. For an ideal fluid one has $c_{\rm vis}^2 = 0$ instead of $1/3$ as for neutrinos. The interaction rate between dark gluons is approximately given by

$$\tau^{-1} \sim \alpha_d^2 T_d, \qquad (7)$$

and one sees that as long as $\alpha_d \gtrsim 10^{-13}$ this rate is larger than H during recombination. Thus on the time scale set by Hubble the dark gluons behave as a perfect fluid. Qualitatively, the interactions reduce the damping of overdensities from relativistic particles streaming out of gravitational potential wells. This has the effect that the CMB peaks are not as suppressed as they would be in the case of additional free-streaming dark radiation.

The Planck Collaboration has performed a fit for $c_{\rm eff}^2$ and $c_{\rm vis}^2$ with $N_{\rm eff}$ fixed to the SM value 3.046, i.e. no additional dark radiation, and found that the parameters were in perfect agreement with the expected value for neutrinos, $c_{\rm eff}^2 = c_{\rm vis}^2 = 1/3$. However, Planck has not yet performed a fit for additional radiation $\triangle N_{\rm eff}$ which is allowed to have nonstandard values for $c_{\rm eff}$ and $c_{\rm vis}$. In particular, if future CMB experiments find evidence for a nonzero $\triangle N_{\rm eff}$ then measuring $c_{\rm vis}$ of this extra component would allow one to distinguish between dark gluons and free-streaming dark radiation, like dark photons or sterile neutrinos [18,19].
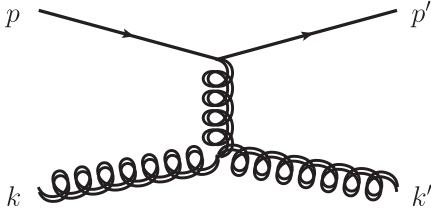
FIG. 6.   t-channel scattering of dark matter with dark gluons.

V. DARK MATTER DARK GLUON INTERACTIONS AND LARGE SCALE STRUCTURE

In this section we study how interactions between dark gluons and DM affect the linear evolution of DM overdensities. The interactions have two important effects. One is the transfer of kinetic energy (i.e. temperature) from the DR to the DM. The other is that DM particles moving through the DR fluid experience a drag force. This drag slows the growth of large scale structures through gravitational clustering. Both rates can be computed by considering scattering of dark gluons with DM particles. The process is a generalization of Compton scattering to the non-Abelian case. The most important new feature is that scattering is dominated by the t-channel diagram shown in Fig. 6 which is divergent for small angle scattering and which only exists for non-Abelian gauge bosons. As we will see, this interaction leads to interesting signatures in large scale structure which distinguish our scenario from other models with interactions between DR and DM (see e.g. [19,47]). In particular, for $\alpha_d \lesssim 10^{-8.5}$ our model predicts a smooth suppression of the matter power spectrum at all scales which could resolve the conflict between the indirect measurement of σ_8 from Planck [1] and the direct measurement from BOSS [6].

To simplify the calculation of the energy transfer rate we consider the limit in which the DM temperature is negligible so that we can take the DM particles to be at rest. We then compute the rate of energy transfer to the DM from scattering [48,49] with a thermal bath of dark gluons. As in the well-known case of Coulomb scattering the cross section is dominated by small-angle forward scattering. To significantly impact the energy of a massive DM particle many collisions with the gluons are required. The collisions are uncorrelated so that the resulting momentum of the DM particle performs a random walk with

$$E = \frac{p^2}{2M_\chi} \simeq \frac{N}{2M_\chi}(\delta p)^2 \simeq \frac{1}{2M_\chi}\sum(\delta p)^2.$$

Here δp is the typical momentum transfer in a single collision and N is the number of collisions. After many such random scatters the resulting DM particle distribution is thermal, but not necessarily with the temperature of the gluon bath. The DM temperature depends on the relative

size of the Hubble expansion rate and the energy transfer rate.

The rate of energy transfer is calculated by averaging the energy transfer per collision over the initial Bose-Einstein distribution of the dark gluons

$$\dot{E} = a\int \frac{d^3k}{(2\pi)^3}2(N^2-1)f(k)\frac{1}{4E_p k}$$

$$\times \int \frac{d^3k'}{(2\pi)^3 2k'}\frac{d^3p'}{(2\pi)^3 2E'_p}(2\pi)^4\delta(p+k-p'-k')$$

$$\times |\bar{M}|^2(E'_p - E_p)(1+f(k')). \tag{8}$$

Here—and for the remainder of this section—time derivatives are taken with respect to conformal time which is the origin of the scale factor a on the right-hand side. Also, $f(k) = 1/(\exp(k/T_{\rm dr} - 1)$ is the gluon thermal distribution function and it is multiplied by $2(N^2-1)$ for the spin and color of the initial gluon. The $1+f(k')$ final state factor accounts for stimulated emission. Finally, the color and spin summed and averaged matrix element (keeping only the t channel) is given by

$$|\bar{M}|^2 = \frac{1}{2}4g_d^4\frac{(s-M_\chi^2)(M_\chi^2-u)}{t^2},$$

where the $1/2$ is the disappointingly boring color factor of the t-channel diagram and s, t, and u are the Mandelstam variables. The integrals are straightforward to evaluate for $p = (M_\chi, \bar{0})$ and give

$$\dot{E} = a(N^2-1)\frac{\pi}{3}\alpha_d^2\log(\alpha_d^{-1})\frac{T_{\rm dr}^3}{M_\chi}$$

$$= a\frac{5}{\pi}\alpha_d^2\log(\alpha_d^{-1})\frac{\rho_{\rm dr}}{T_{\rm dr}M_\chi}. \tag{9}$$

One subtlety one encounters is a logarithmic divergence at small t which stems from the long range of the interaction mediated by a massless gluon. In the thermal plasma of gluons the interaction range is made finite by screening. This effect can be parametrized by including a Debye mass for the gluon, $m_{\rm Debye}^2 \sim g_d^2 T_{\rm dr}^2$ [50]. With the Debye mass the logarithmic divergence becomes the $\log(\alpha_d^{-1})$ in Eq. (9). This is analogous to the ubiquitous "Coulomb logarithm" in plasma physics.

Using $T = 2/3E$ we obtain an equation for the evolution of dark matter temperature [51],

$$\dot{T}_\chi = -2\frac{\dot{a}}{a}T_\chi + a(N^2-1)\frac{2\pi}{9}\alpha_d^2\log(\alpha_d^{-1})\frac{T_{\rm dr}^2}{M_\chi}(T_{\rm dr}-T_\chi),$$

$$\tag{10}$$

where the $T_{\rm dr} - T_\chi$ factor generalizes the energy transfer rate in Eq. (9) to the case in which the thermal motion of the DM is not negligible. To understand the possible solutions to this equation one compares the size of the temperature
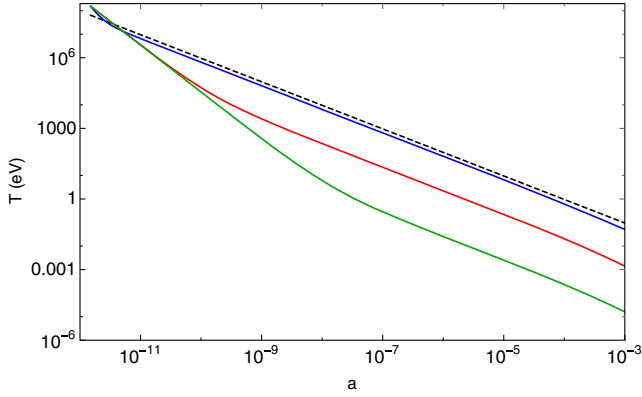
FIG. 7 (color online). Dark sector temperatures as a function of scale factor a. Shown are the dark gluon temperature (black dashed), and DM temperatures for three representative values of $\alpha_d = 10^{-8}$ (upper, blue), $\alpha_d = 10^{-9}$ (middle, red), and $\alpha_d = 10^{-10}$ (lower, green).

transfer term with the Hubble redshift term $\dot{a}/a T_\chi \sim a T_\chi T^2/M_{\text{Planck}}$ (during radiation domination). For large temperature transfer rates DM and DR are kept in thermal equilibrium by the interactions and $T_\chi = T_{\text{dr}}$. Note that both terms scale with the cube of the temperature; thus if DM and DR are in equilibrium at one temperature they will be in equilibrium throughout radiation domination.

For couplings $\alpha_d < 10^{-8}$ and assuming comparable starting temperatures $T_\chi \sim T_{\text{dr}}$, the Hubble term initially dominates over the interaction term and the DM temperature plummets relative to the temperature of radiation: $T_\chi \sim a^{-2}$ vs $T_{\text{dr}} \sim a^{-1}$. This is the regime where our DM behaves like ordinary CDM. However, note that the Hubble term scales proportional to $T_{\text{dr}}^2 T_\chi$ whereas the collision term scales like T_{dr}^3. Thus for sufficiently small T_χ the two terms become comparable and the DM temperature switches to scaling proportional to a^{-1}, keeping the ratio T_χ/T_{dr} constant. In Fig. 7 we show numerical solutions for the DM temperature as a function of scale factor for three representative values of α_d.

For values of α_d for which DM and DR are in thermal equilibrium DM behaves very differently from ordinary CDM. The pressure from the dark gluons prevents the growth of DM overdensities during radiation domination. This can be seen as the sharp drop in the DM power spectrum in Fig. 8. For smaller values of α_d the dark gluons still influence the evolution of DM overdensities; however the effects are more subtle and we employ the formalism of Ma and Bertschinger [51] to study them.

Following [51] we write down the linearized evolution equations for overdensities including the interactions between the DM and DR fluids in conformal Newtonian gauge. To avoid the complications of solving a full Boltzmann code we work with a simplified scenario. We replace all relativistic energy density in the SM (i.e. neutrinos and photons) with an identical energy density
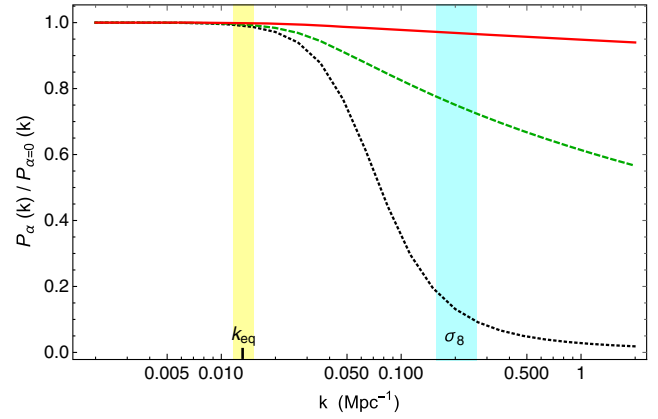

FIG. 8 (color online). Power spectrum including the DM-DR interactions normalized by the power spectrum with interactions turned off. The black dotted curve corresponds to $\alpha_d = 10^{-8}$, the green dashed curve corresponds to $\alpha_d = 10^{-8.5}$, and the red line corresponds to $\alpha_d = 10^{-9}$. The power spectra are defined proportional to δ_{DM}^2 at $a = 10^{-3}$. The vertical yellow band labeled k_{eq} indicates modes which enter the horizon at matter-radiation equality; modes which enter the horizon earlier are to the right (larger k). The blue band labeled σ_8 indicates modes which the observable σ_8 is most sensitive to.

which is made up of only photons. And we replace all matter (dark matter and baryons) with an equivalent energy density of only dark matter. In addition, we approximate by treating the photons as a perfect fluid (zero viscosity). This is only true before recombination but soon after recombination photons contribute only a negligible amount to the energy density and thus to the evolution of DM overdensities. Since our goal is to demonstrate the effect of the interactions on the DM density perturbations we compare our scenario with interactions to the same scenario with $\alpha_d = 0$.

In Fourier space the equations for the DM and DR overdensities are

$$\dot{\delta}_{\text{DM}} = -\theta_{\text{DM}} + 3\dot{\psi}$$

$$\dot{\theta}_{\text{DM}} = -\frac{\dot{a}}{a}\theta_{\text{DM}} + a\tau_c^{-1}(\theta_{\text{DR}} - \theta_{\text{DM}}) + k^2\psi$$

$$\dot{\delta}_{\text{DR}} = -\frac{4}{3}\theta_{\text{DR}} + 4\dot{\psi}$$

$$\dot{\theta}_{\text{DR}} = k^2\frac{\delta_{\text{DR}}}{4} + k^2\psi + \frac{3}{4}\frac{\rho_{\text{DM}}}{\rho_{\text{DR}}}a\tau_c^{-1}(\theta_{\text{DM}} - \theta_{\text{DR}})$$

$$\dot{\delta}_\gamma = -\frac{4}{3}\theta_\gamma + 4\dot{\psi}$$

$$\dot{\theta}_\gamma = \frac{1}{4}k^2\delta_\gamma + k^2\psi$$

$$k^2\psi + 3\frac{\dot{a}}{a}\left(\dot{\psi} + \frac{\dot{a}}{a}\psi\right) = -\frac{a^2}{2M_{\text{Pl}}^2}\sum_i \rho_i\delta_i, \qquad (11)$$

where the dots represent derivatives with respect to conformal time, ρ_X is the average energy density of fluid

X, and δ_X and θ_X are related to the overdensity and velocity divergence in fluid X. We have also set the two metric perturbations ψ and ϕ equal because we are treating the photons and dark radiation as ideal fluids (no anisotropic stress) and did not include neutrinos which have sizable anisotropic stresses. The interaction between dark matter and dark radiation is encoded in the momentum transfer rate τ_c^{-1} [49]. It is defined as the change in momentum $\dot{\vec{p}}_\chi = -a\tau_c^{-1}\vec{p}_\chi$ which a DM particle with momentum $\vec{P}$ experiences due to friction as it is moving through the dark gluon fluid. Microscopically, the friction arises from collisions between DM particles and dark gluons and to compute it we evaluate

$$\dot{\vec{p}} = a \int \frac{d^3k}{(2\pi)^3} f(k) \frac{1}{4E_p k} \int \frac{d^3k'}{(2\pi)^3 2k'} \frac{d^3p'}{(2\pi)^3 2E'_p} (2\pi)^4$$
$$\times \delta(p+k-p'-k')|M|^2(\vec{p}'-\vec{p})(1+f(k')), \quad (12)$$

where now the initial DM momentum $\vec{p}$ is nonzero and we expand to first order in p/M_χ. Employing the same approximations as for the energy transfer rate we obtain

$$\tau_c^{-1} = (N^2-1)\frac{\pi}{9}\alpha_d^2 \log \alpha_d^{-1} \frac{T_{\rm dr}^2}{M_\chi}. \quad (13)$$

We integrate the equations for the overdensities from $a = 10^{-7}$, when all modes of interest are well outside the horizon, until $a = 10^{-3}$. We use initial conditions corresponding to adiabatic perturbations:

$$\delta_\gamma = \delta_{\rm DR} = \frac{4}{3}\delta_{\rm DM} = -2\psi = C(k), \quad (14)$$

where the initial perturbations $C(k) \sim k^{-3/2}$ are determined by the physics of inflation. We define the DM power spectrum equal to the square of the perturbations, $P(k) \equiv \delta_{\rm DM}^2$, at scale factor $a = 10^{-3}$. To focus only on effects of the coupling between DM and DR we form a ratio where we divide the power spectrum with interactions turned on by the power spectrum with $\alpha_d = 0$. Note that since the equations are linear the initial values for the perturbations, $C(k)$, drop out in the ratio.

The ratios of power spectra for different values of α_d are plotted in Fig. 8. For the plot we chose the number of colors $N = 2$ and $M_\chi = 1.2$ TeV. One sees that for $\alpha_d = 10^{-8}$ the power spectrum is strongly suppressed for modes which entered the horizon before matter-radiation equality. These are modes with $k > k_{\rm eq} \sim 0.015$ Mpc^{-1}. This should be expected because in this case the DM is in equilibrium with the DR bath throughout radiation domination. For the smaller values of $\alpha_d = 10^{-8.5}$ and 10^{-9} the power spectrum is less affected with modes which entered the horizon earlier (larger k) suppressed more that those which entered later. Modes which enter the horizon after matter-radiation equality are not suppressed for any of the couplings plotted.

The light blue vertical band indicates the range of modes which the observable σ_8 is sensitive to (σ_8 is a measurement of the matter fluctuations in spheres of radius of $8h^{-1}$ Mpc).

The smooth suppression of power at all scales that we are finding is special to our scenario and stems from the fact that the momentum transfer rate scales with temperature as $T_{\rm dr}^2$, the same scaling as Hubble. Thus it is possible to arrange for the couplings to have a small effect but act over a large range of scales. This should be contrasted with cases where the interactions scale like a higher power of $T_{\rm dr}$ in which case they are important at high scales and have no effect at low scales. In such scenarios the power spectrum has a sharp cutoff at scales of the size of the horizon at the time when the interactions cease to be important, leaving larger scales unaffected and wiping out the smaller scales that entered the horizon at earlier times.

The smooth suppression of power is exciting because it might help resolve two sources of tension in recent experimental results. A fit to the most recent Planck CMB data is used to fix the parameters of ΛCDM. Using the model, the Planck collaboration predicts $\sigma_8^{\Lambda\rm CDM} = 0.829 \pm 0.014$ ("TT + lowP," 1σ errors). This value is about 2σ higher than direct measurements of large scale structure [1,6,7] (for example, gravitational lensing of the CMB as measured by Planck gives $\sigma_8^{\rm lensing} = 0.802 \pm 0.012$). A reduction of the predicted power spectrum due to DM-DR interactions as it occurs in our model for $\alpha_d \sim 10^{-9}$ removes this tension between the Planck fit and LSS data. Interestingly, the tension in σ_8 is currently also driving the Planck fit for $N_{\rm eff}$ and H_0 to lower values because in ΛCDM larger values for those parameters would correlate with even larger values for σ_8. Thus after including DM-DR interactions the Planck fit might prefer $N_{\rm eff} > 3$ which would create more room for dark gluons. Furthermore, larger $N_{\rm eff}$ is correlated in the ΛCDM fit with a larger value for H_0 (to keep the position of the acoustic peaks in the CMB fixed [1,44–46]). This in turn would allow better agreement between the H_0 values from Planck and supernova data [1], another area of mild tension in cosmological data. Clearly, a more quantitative analysis of this issue is desirable and requires including the non-Abelian dark radiation in a full Boltzmann code.

VI. CONCLUSIONS

In this work we have studied a new type of dark sector with massless non-Abelian gauge bosons superweakly coupled to the DM. There are many different possibilities for the DM coupling to the standard model. As an example, we chose our DM particle to transform as $SU(2)_{\rm weak}$ triplets and fundamentals under the dark $SU(N)_d$ gauge group.

Our model has three new parameters, the coupling constant α_d, the mass of the DM particles M_χ, and the size of the gauge group N. Demanding the correct DM abundance from thermal freeze-out fixes the DM mass in terms of N, thus leaving a two-dimensional parameter

space. Constraints on this parameter space can be derived from several different experiments.

The first set of constraints derives simply from the multiplicity of the dark matter and would even apply if the dark coupling constant were zero. The multiplicity of dark matter affects the usual WIMP searches (direct and indirect detection and collider searches). The effect is simply that dark color multiplicity factors enhance pair production and decrease pair annihilation. Therefore the DM mass required in order to predict the right DM abundance decreases by $\sqrt{2N}$. It also increases the collider cross section, placing this type of dark matter within easy reach of the proposed 100 TeV collider. The decrease in mass and in annihilation cross section also removes the current tension between thermally produced $SU(2)_{\text{weak}}$ triplet dark matter and H.E.S.S data. Despite the decrease in annihilation cross section, the $SU(2)_{\text{weak}}$ triplet DM model annihilation cross section is within the projected reach for CTA.

For $\alpha_d \gtrsim 10^{-13}$ the dark gluons thermalize with the SM in the early Universe and contribute to dark radiation. The limits placed on N_{eff} from Planck constrain N to be at most 3. However, the self interactions of the dark gluons leave an imprint in the CMB which is distinct from that of free-streaming fluids like neutrinos or dark photons. This can be used to distinguish between the two types of radiation if future experiments establish the need for a nonstandard contribution to N_{eff}.

Finally we studied the effects of the interactions between DM and DR on the power spectrum. We found that for $\alpha_d \gtrsim 10^{-8}$ the interactions strongly suppress the power spectrum of modes entering the horizon before matter-radiation equality and thus such couplings are ruled out. On the other hand, for $\alpha_d \lesssim 10^{-8.5}$ the interactions predict a smooth decrease in the power spectrum, which can potentially solve the discrepancy between Planck and large scale structure data and the discrepancy between Planck and supernova measurements of H_0. We hope to return to this in future work.

[1] P. Ade *et al.* (Planck Collaboration), Planck 2015 results. XIII. Cosmological parameters, arXiv:1502.01589.

[2] J. L. Feng, H. Tu, and H.-B. Yu, Thermal relics in hidden sectors, J. Cosmol. Astropart. Phys. 10(2008) 043.

[3] J. L. Feng, M. Kaplinghat, H. Tu, and H.-B. Yu, Hidden charged dark matter, J. Cosmol. Astropart. Phys. 07 (2009) 004.

[4] U. Frana, R. A. Lineros, J. Palacio, and S. Pastor, Probing interactions within the dark matter sector via extra radiation contributions, Phys. Rev. D **87**, 123521 (2013).

[5] A. G. Riess, L. Macri, S. Casertano, H. Lampeitl, H. C. Ferguson, A. V. Filippenko, S. W. Jha, W. Li, and R. Chornock, A 3telescope and wide field camera 3, Astrophys. J. **730**, 119 (2011).

[6] F. Beutler *et al.* (BOSS Collaboration), The clustering of galaxies in the SDSS-III baryon oscillation spectroscopic survey: signs of neutrino mass in current cosmological data sets, Mon. Not. R. Astron. Soc. **444**, 3501 (2014).

[7] R. A. Battye, T. Charnock, and A. Moss, Tension between the power spectrum of density perturbations measured on large and small scales, Phys. Rev. D **91**, 103508 (2015).

[8] L. B. Okun, Theta particles, Nucl. Phys. **B173**, 1 (1980).

[9] L. B. Okun, Thetons, JETP Lett. **31**, 144 (1980).

[10] M. Yu. Khlopov, On relic θ-matter, Sov. J. Nucl. Phys. **32**, 828 (1980).

[11] J. Kang and M. A. Luty, Macroscopic strings and "quirks" at colliders, J. High Energy Phys. 11 (2009) 065.

[12] J. L. Feng and Y. Shadmi, WIMPless dark matter from non-Abelian hidden sectors with anomaly-mediated supersymmetry breaking, Phys. Rev. D **83**, 095011 (2011).

[13] K. S. Jeong and F. Takahashi, Self-interacting dark radiation, Phys. Lett. B **725**, 134 (2013).

[14] S. Baek, P. Ko, and W.-I. Park, Hidden sector monopole, vector dark matter, and dark radiation with Higgs portal, J. Cosmol. Astropart. Phys. 10(2014) 067.

[15] K. K. Boddy, J. L. Feng, M. Kaplinghat, and T. M. P. Tait, Self-interacting dark matter from a non-Abelian hidden sector, Phys. Rev. D **89**, 115017 (2014).

[16] N. Blinov, J. Kozaczuk, A. Menon, and D. E. Morrissey, Confronting the moduli-induced lightest-superpartner problem, Phys. Rev. D **91**, 035026 (2015).

[17] N. Yamanaka, S. Fujibayashi, S. Gongyo, and H. Iida, Dark matter in the hidden gauge theory, arXiv:1411.2172.

[18] A. Friedland, K. M. Zurek, and S. Bashinsky, Constraining models of neutrino mass and neutrino interactions with the Planck satellite, arXiv:0704.3271.

[19] R. Diamanti, E. Giusarma, O. Mena, M. Archidiacono, and A. Melchiorri, Dark radiation and interacting scenarios, Phys. Rev. D **87**, 063509 (2013).

[20] C. Brust, D. E. Kaplan, and M. T. Walters, New light species and the CMB, J. High Energy Phys. 12 (2013) 058.

[21] S. Hofmann, D. J. Schwarz, and H. Stoecker, Damping scales of neutralino cold dark matter, Phys. Rev. D **64**, 083507 (2001).

[22] A. Loeb and M. Zaldarriaga, The small-scale power spectrum of cold dark matter, Phys. Rev. D **71**, 103520 (2005).

[23] E. Bertschinger, The effects of cold dark matter decoupling and pair annihilation on cosmological perturbations, Phys. Rev. D **74**, 063509 (2006).

[24] H.-C. Cheng, B. A. Dobrescu, and K. T. Matchev, Generic and chiral extensions of the supersymmetric standard model, Nucl. Phys. **B543**, 47 (1999).

[25] M. Ibe, S. Matsumoto, and R. Sato, Mass splitting between charged and neutral winos at two-loop level, Phys. Lett. B **721**, 252 (2013).

[26] M. Cirelli, N. Fornengo, and A. Strumia, Minimal dark matter, Nucl. Phys. **B753**, 178 (2006).

[27] E. W. Kolb and M. S. Turner, The early Universe, Front. Phys. **69**, 127 (1990).

[28] M. Cirelli, A. Strumia, and M. Tamburini, Cosmology and astrophysics of minimal dark matter, Nucl. Phys. **B787**, 152 (2007).

[29] R. J. Hill and M. P. Solon, WIMP-Nucleon Scattering with Heavy WIMP Effective Theory, Phys. Rev. Lett. **112**, 211602 (2014).

[30] P. Cushman, C. Galbiati, D. McKinsey, H. Robertson, T. Tait *et al.*, Working Group report: WIMP dark matter direct detection, arXiv:1310.8327.

[31] T. Cohen, M. Lisanti, A. Pierce, and T. R. Slatyer, Wino dark matter under siege, J. Cosmol. Astropart. Phys. 10 (2013) 061.

[32] J. Fan and M. Reece, In wino veritas? Indirect searches shed light on neutralino dark matter, J. High Energy Phys. 10 (2013) 124.

[33] M. Bauer, T. Cohen, R. J. Hill, and M. P. Solon, Soft collinear effective theory for heavy WIMP annihilation, J. High Energy Phys. 01 (2015) 099.

[34] G. Ovanesyan, T. R. Slatyer, and I. W. Stewart, Heavy Dark Matter Annihilation from Effective Field Theory, Phys. Rev. Lett. **114**, 211302 (2015).

[35] M. Baumgart, I. Z. Rothstein, and V. Vaidya, Constraints on galactic wino densities from gamma ray lines, J. High Energy Phys. 04 (2015) 106.

[36] S. Funk, Indirect detection of dark matter with gamma rays, arXiv:1310.2695.

[37] G. Aad *et al.* (ATLAS Collaboration), Search for new phenomena in final states with an energetic jet and large missing transverse momentum in pp collisions at $\sqrt{s} = 8$ TeV with the ATLAS detector, Eur. Phys. J. C **75**, 299 (2015).

[38] V. Khachatryan *et al.* (CMS Collaboration), Search for dark matter, extra dimensions, and unparticles in monojet events in proton-proton collisions at $\sqrt{s} = 8$ TeV, Eur. Phys. J. C **75**, 235 (2015).

[39] J. Alwall, M. Herquet, F. Maltoni, O. Mattelaer, and T. Stelzer, MadGraph 5: Going beyond, J. High Energy Phys. 06 (2011) 128.

[40] M. Low and L.-T. Wang, Neutralino dark matter at 14 TeV and 100 TeV, J. High Energy Phys. 08 (2014) 161.

[41] M. Cirelli, F. Sala, and M. Taoso, Winolike minimal dark matter and future colliders, J. High Energy Phys. 01 (2015) 041.

[42] D. S. M. Alves, J. Galloway, J. T. Ruderman, and J. R. Walsh, Running electroweak couplings as a probe of new physics, J. High Energy Phys. 02 (2015) 007.

[43] G. Mangano, G. Miele, S. Pastor, and M. Peloso, A precision calculation of the effective number of cosmological neutrinos, Phys. Lett. B **534**, 8 (2002).

[44] W. Hu, D. J. Eisenstein, M. Tegmark, and M. J. White, Observationally determining the properties of dark matter, Phys. Rev. D **59**, 023512 (1998).

[45] R. Bowen, S. H. Hansen, A. Melchiorri, J. Silk, and R. Trotta, The impact of an extra background of relativistic particles on the cosmological parameters derived from microwave background anisotropies, Mon. Not. R. Astron. Soc. **334**, 760 (2002).

[46] S. Bashinsky and U. Seljak, Neutrino perturbations in CMB anisotropy and matter clustering, Phys. Rev. D **69**, 083002 (2004).

[47] R. J. Wilkinson, C. Boehm, and J. Lesgourgues, Constraining dark matter-neutrino interactions using the CMB and large scale structure, J. Cosmol. Astropart. Phys. 05 (2014) 011.

[48] S. D. McDermott, H.-B. Yu, and K. M. Zurek, Turning off the lights: How dark is dark matter? Phys. Rev. D **83**, 063509 (2011).

[49] C. Dvorkin, K. Blum, and M. Kamionkowski, Constraining dark matter-baryon scattering with linear cosmology, Phys. Rev. D **89**, 023519 (2014).

[50] P. B. Arnold and L. G. Yaffe, The non-Abelian Debye screening length beyond leading order, Phys. Rev. D **52**, 7208 (1995).

[51] C.-P. Ma and E. Bertschinger, Cosmological perturbation theory in the synchronous and conformal Newtonian gauges, Astrophys. J. **455**, 7 (1995).